Desalination and Water Treatment
www.deswater.com

doi: 10.1080/19443994.2015.1107755

57 (2016) 20401–20410
September

Taylor & Francis
Taylor & Francis Group

Arsenate removal from groundwater by modified alkaline residue

Yubo Yan[a,b], Can Chen[c], Qiao Li[a,b], Xiuyun Sun[a,b,*], Lianjun Wang[a,b,*]

[a]*School of Environmental and Biological Engineering, Nanjing University of Science & Technology, Nanjing 210094, China, emails: yyb0920@sina.com (Y. Yan), 790942369@qq.com (Q. Li), sunxyun@njust.edu.cn (X. Sun), wanglj@njust.edu.cn (L. Wang)*
[b]*Jiangsu Key Laboratory of Chemical Pollution Control and Resources Reuse, Nanjing 210094, China*
[c]*Institute of Environment Engineering Technology, Guangdong Provincial Academy of Environmental Science, Guangzhou 510045, China, email: chen0701040103@qq.com*

Received 26 April 2015; Accepted 7 October 2015

ABSTRACT

Alkaline residue, a common solid waste from the Lianyungang Soda Plant, China, was, respectively, modified by $FeCl_3{\cdot}6H_2O$ (FeCAR) and $MnSO_4{\cdot}H_2O$ (MnCAR) for arsenate adsorption. The specific surface areas and morphologies of FeCAR and MnCAR were determined by BET and SEM methods. The adsorption properties including adsorption kinetics, isotherms, and thermodynamics were investigated in depth. The experimental data were analyzed by different kinetic and isotherm models, and the results showed that for both FeCAR and MnCAR, the pseudo-second-order kinetic model was the best-fit model for describing the adsorption process while the Langmuir isotherm model provided the best fit to the equilibrium data. The maximum adsorption capacity calculated from the Langmuir equation was 44.4 mg/g for FeCAR and 22.6 mg/g for MnCAR, which were greater than other low-cost materials. The positive value of ΔH° indicated that the arsenate adsorption on adsorbents was endothermic, which was supported by the increasing adsorbed amount of arsenate with temperature. The positive value of ΔS° reflected good affinity of arsenate toward the modified alkaline residue. Overall, alkaline residue modified by iron or manganese was a very promising alternative adsorbent for removing arsenate from groundwater.

Keywords: Alkaline residue; Modification; Adsorption; Arsenate

1. Introduction

In recent years, environmental (particularly groundwater and soil) pollution by arsenic (As) has attracted global attention because of its ubiquitous nature and high toxicity. Naturally, the existence of arsenic in the environment is mostly due to weathering and erosion of rocks and soils and volcanic emissions [1]. Anthropogenic sources such as biological and mining activities, combustion of fossil fuels, waste disposal, and indiscriminate use of arsenic pesticides, herbicides, and wood preservatives make the problem more serious for animals and human beings [2]. It was reported that around 150 million people from over 70 countries and regions were suffering from arsenic pollution, with more than 70% of the population living in Asia, especially in China, Bangladesh, Vietnam, and India [3]. Long-term exposure to drinking water with even a very low arsenic concentration (0.01–0.05 mg/L) can result in severe health problems including hypertension, high risk of cancers (e.g. skin, lung, or bladder), and cardiovascular or peripheral vascular

*Corresponding authors.

diseases [4,5]. In view of the negative effects of arsenic on humans and based on the epidemiological data from Taiwan, in 1993, the World Health Organization recommended that the maximum permitted concentration of arsenic in drinking water be reduced to 10 μg/L [6]. Therefore, developing technologies to efficiently remove arsenic from drinking water sources are urgently and universally required.

The conventional technologies for the removal of arsenic from aqueous solution include oxidation/precipitation, coagulation/coprecipitation, nanofiltration, reverse osmosis, solvent extraction, ion exchange, adsorption, foam flotation, biological process, and electrocoagulation [7]. Comparing with these technologies, adsorption by various low-cost adsorbents is considered to be very promising due to its high-removal efficiency, economics, and ease of operation. For example, Tu et al. [8] have successfully recycled the copper ferrite, printed circuit board sludge for the removal of arsenate from wastewater. Chen et al. [3] developed the ferric-impregnated volcanic ash for arsenate(V) removal from an aqueous medium. Markovski et al. [6] found that the eggshell modified by goethite and α-MnO_2 possessed greater adsorption capacity for arsenate than that modified by goethite or α-MnO_2.

Alkaline residue, a common waste solid, is the by-product of the ammonia–soda process for the production of soda ash. Every year in China, a large portion of alkaline residue is used in cement production and road construction, but still a considerable portion of alkaline residue is disposed directly into open dumps or landfills [9]. Thus, finding a potential market to reuse alkaline residue may be an economically valuable solution to this problem. During the past decade, many researchers focused on applying alkaline residue for removing anionic dyes [10,11], heavy metals [12], and ammonium [13] from wastewater.

At this current time, there are no reports published regarding modifying alkaline residue with iron or manganese for arsenate removal from groundwater. The significance of this work is to develop special interest composite adsorbent materials based on alkaline residue, calcined and modified in order to gain novel naturally based adsorbents of the optimal morphological properties, enhanced affinity and reactivity toward arsenate, and expecting to be economically viable and reliable for the treatment of polluted groundwater. Therefore, the objectives of this work were (a) to explore the feasibility of using iron- or manganese-modified calcined alkaline residue to remove arsenate from groundwater, (b) to thoroughly investigate the adsorbents' adsorption performance, including pH impact, adsorption kinetics, isotherm, and thermodynamics, and (c) to evaluate the effect of common coexisting ions on the removal of arsenate.

2. Materials and methods

2.1. Materials

Alkaline residue was collected from Lianyungang Soda Ash Plant, China. Prior to use, the raw sample was subjected to some conventional pretreatment processes. Briefly, the sample was washed thoroughly in deionized water to remove soluble salts, dried at 105°C for 24 h to a constant weight, sieved to obtain fine powder (particle size < 0.15 mm). The dried powder sample was then calcined at 800°C in an electric furnace under air atmosphere. Finally, the cooled sample was stored in a desiccator for the preparation of adsorbents. The major composition of obtained sample was identified by X-ray fluorescence spectrometer (XRF) (XRF-1800, Shimadzu, Japan) and the results were CaO (58.73 wt.%), MgO (14.25 wt.%), SiO_2 (11.16 wt.%), Fe_2O_3 (4.32 wt.%), and Al_2O_3 (3.97 wt.%). An arsenate working stock solution (1,000 mg/L As, pH 7.0 ± 0.05) was prepared by dissolving appropriate amounts of $Na_2HAsO_4{\cdot}7H_2O$ in Milli-Q water. The desired concentrations in experimental processes were obtained by diluting the stock solution. All chemicals and reagents used were purchased from Nanjing Chemical Reagent Company and were of analytical grade.

2.2. Adsorbent preparation and characterization

For the preparation of iron-modified alkaline residue, 50 g of calcined alkaline residue was treated with 500 mL of 1 M $FeCl_3{\cdot}6H_2O$ solution. The mixture was then cured at 100°C for 2 h. After treatment, the solid phase was separated by centrifugation, washed with Milli-Q water, dried at 100°C, and screened through a 100 mesh sieve. The obtained powder was stored in a desiccator and designated as FeCAR. The procedure of manganese-modified alkaline residue followed the same procedure, except 500 mL of 1 M $MnSO_4{\cdot}H_2O$ solution was used instead of $FeCl_3{\cdot}6H_2O$, the obtained powder was named MnCAR.

The specific surface area, pore volume, and pore size distribution of adsorbents were measured by nitrogen adsorption at 77 K (ASAP 2020, Micromeritics Instrument, USA). The morphology of each adsorbent was determined using a scanning electronic microscope coupled with energy dispersive spectroscopy (SEM-EDS) (Quanta 250FEG, FEI, USA).

2.3. Sorption studies

The adsorption experiments of As(V) were carried out according to batch method. The conical flasks containing 0.02 g adsorbent and 50 mL solution at desired As(V) concentration, pH, and temperature were placed in an air bath oscillator with a constant speed of 200 rpm. After adsorption, the mixtures were filtered through a 0.45-μm membrane filter and the filtrates were analyzed for residual As(V) concentration via an inductively coupled plasma optical emission spectrometry (ICP-OES) (Optima 7000DV, Perkin–Elmer, USA). The amount of As(V) adsorption at time t, q_t (mg/g), is calculated based on:

$$q_t = \frac{(C_0 - C_t)V}{m} \quad (1)$$

where C_0 and C_t (mg/L) are the As(V) concentration in the initial solution and at time t, respectively, V (L) is the volume of solution, and m (g) is the weight of the adsorbent added to the solution.

For determination of pH impact on adsorption, the pH of 15 mg/L As(V)-simulated polluted groundwater was adjusted using 0.1 M NaOH or 0.1 M HNO_3. Adsorption kinetics of As(V) was studied in the range of 10–600 min at pH 7.2 ± 0.1. Adsorption isotherm was investigated in the range of 0.5–20 mg/L. Adsorption thermodynamics study was carried out with 10 mg/L As(V) solution at 25, 35, and 45˚C, respectively.

3. Results and discussion

3.1. Characterization of FeCAR and MnCAR

3.1.1. Before adsorption

Fig. 1 exhibits the textural properties of FeCAR and MnCAR. According to the pore size, the International Union of Pure and Applied Chemistry (IUPAC) classifies the pores into three groups: micropore (<2 nm), mesopore (2–50 nm), and macropore (>50 nm). From Fig. 1(a) and (b), it was found that FeCAR and MnCAR both contained the mesoporous structure. Furthermore, the BET surface areas were 216.7 and 117.0 m^2/g for FeCAR and MnCAR, respectively, which were much higher than other reported adsorption materials, such as fabricated copper ferrite [8] or calcium alginate beads [14]. Overall, the structures of modified alkaline residue were successful for arsenate adsorption. Fig. 2 shows the morphology of FeCAR and MnCAR. The surface of FeCAR was densely covered with regular spherical-shaped nanoparticles (Fig. 2(a)), while irregular rod-shaped particles sporadically dispersed on the surface of MnCAR (Fig. 2(b)). On the other hand, the FeCAR's surface was rougher than MnCAR's. This finding could also be used to explain the differences in specific surface area between FeCAR and MnCAR.

3.1.2. After adsorption

Fig. 3(a) (5,000×) and (b) (20,000×) show the morphology of FeCAR after As(V) adsorption. It can be found that irregular particles dispersed heterogeneously on the surface of the final solid. From Fig. 3(c), the trace of As is observed in related EDS spectrum, confirming that the As was adsorbed on the surface of FeCAR. For MnCAR, the rod-shaped particles disappeared and instead, the agglomerated particle shapes were presented after As(V) adsorption (Fig. 3(d) and (e)). Similarly, the strong peaks of As were observed in related EDS spectrum (Fig. 3(f)), suggesting that the As was also adsorbed on the surface of MnCAR.

3.2. Effect of pH

Considering that the pH value of the natural groundwater commonly ranges from 5.0 to 9.0 [15], 5.0, 7.0, and 9.0 were selected to assess the effect of pH on As(V) adsorption. As indicated in Fig. 4, the uptake of As(V) by FeCAR and MnCAR both show a decrease tendency in As(V) adsorbed amount with the increase in initial solution pH from 5.0 to 9.0, and the amount of As(V) adsorption on FeCAR was higher than that of MnCAR all the time. It can be interpreted by electrostatic attraction between adsorbents and arsenate. The curve of Fig. 4 shows that the surfaces of adsorbents were positively charged at pH ≤ 7.0, which provided more active sites for arsenate. In comparison with MnCAR, FeCAR had a more positive surface at pH ≤ 7.0 and a less negative surface at pH > 7.0, which was benefit for FeCAR to adsorb arsenate.

3.3. Adsorption kinetics

The kinetics of arsenate adsorption on FeCAR and MnCAR are shown in Fig. 5 with an initial As(V) concentration of 10 mg/L. It could be observed that the adsorption of arsenate on FeCAR and MnCAR both consisted of a fast and a slow reaction process. The fast process was completed in approximately 60 min, in which arsenate adsorption increased rapidly with increasing contact time, whereas the slow process could extend to 10 h, in which the increase in arsenate adsorption diminished. This result is in accordance with experiments of other authors [16,17] who also

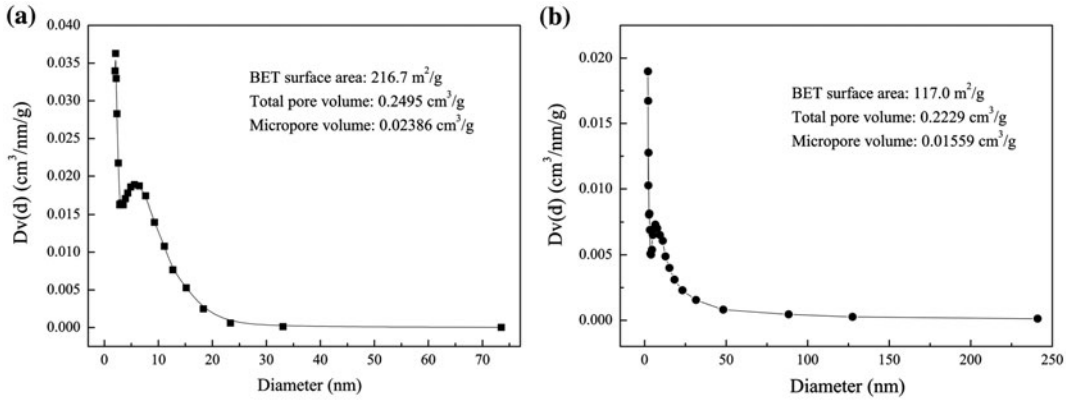

Fig. 1. Textural properties of FeCAR (a) and MnCAR (b).

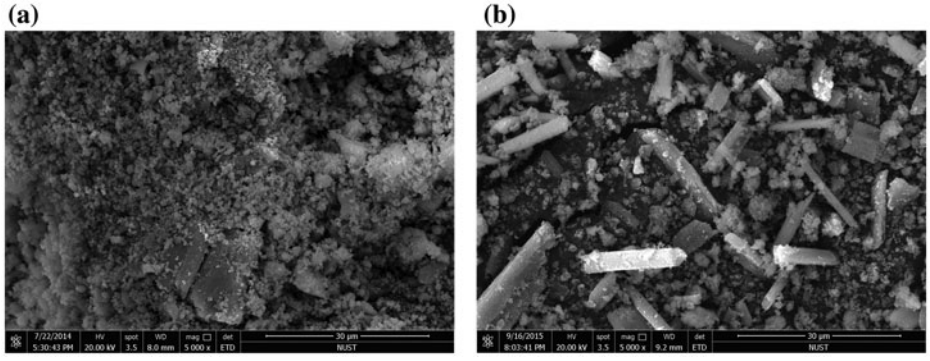

Fig. 2. Scanning electron microscopy (SEM) images of FeCAR (a) and MnCAR (b).

found a two-phase reaction with a rapid first step and a slower second phase. Additionally, the amount of arsenate adsorbed on FeCAR was significantly higher than that of MnCAR, indicating that the affinity between FeCAR and arsenate was greater than MnCAR.

To investigate the mechanism of adsorption and potential rate-controlling steps including mass transport and chemical reaction processes, the pseudo-first-order [18] and pseudo-second-order [19] kinetic models were used to test experimental data. Their linear forms can be expressed as:

$$\text{Pseudo-first-order}: \quad \log(q_e - q_t) = \log q_e - \frac{k_1 t}{2.303} \tag{2}$$

$$\text{Pseudo-second-order}: \quad \frac{t}{q_t} = \frac{1}{k_2 q_e^2} + \frac{t}{q_e} \tag{3}$$

where q_e and q_t (mg/g) are the amount of arsenate adsorbed at equilibrium and at time t (min), k_1 (min^{-1}) and k_2 (g/(mg min)) are the rate constants for the pseudo-first order and pseudo-second order, respectively. Furthermore, when $t \to 0$, the initial adsorption rate (h mg/(g min)) of arsenate on FeCAR or MnCAR can also be defined by the following equation:

$$h = k_2 q_e^2 \tag{4}$$

As can be seen from Fig. 6 and Table 1, the correlation coefficients (R^2) of the pseudo-first-order kinetic model (0.9397 for FeCAR and 0.9383 for MnCAR) are lower than the results obtained from the pseudo-second-order kinetic model (0.9999 for FeCAR and 0.9995 for MnCAR). In addition, the theoretical q_e values calculated from the pseudo-first-order equation (3.54 mg/g for FeCAR and 4.85 mg/g for MnCAR) are evidently less than the experimental values (24.9 mg/g for FeCAR and 18.2 mg/g for MnCAR) while the results from the pseudo-second-order equation (25.1 mg/g for FeCAR and 18.4 mg/g for MnCAR) are very close to

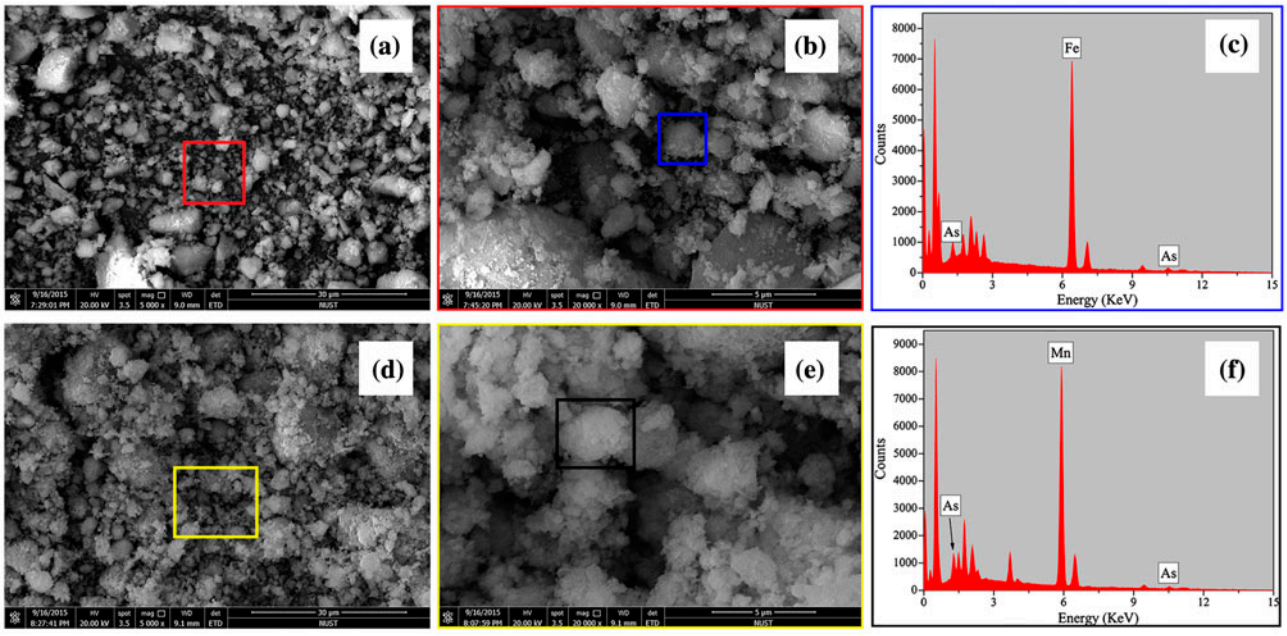

Fig. 3. Scanning electron microscopy (SEM) images and energy dispersive spectra (EDS) of the final solid after As(V) adsorption onto FeCAR (a–c) and MnCAR (d–f).

the experimental values. Therefore, the pseudo-second-order model is the preferred model choice to describe the adsorption systems. This also suggests that a chemisorption reaction occurs between arsenate and the surface of adsorbents. Moreover, the adsorption rate of arsenate on FeCAR (6.91 mg/(g min)) was faster than that of MnCAR (1.95 mg/(g min)), which is consistent with the tendency observed from Fig. 5.

3.4. Adsorption isotherms

Adsorption equilibrium data, expressed by the mass of adsorbate adsorbed per unit weight of adsorbent and liquid phase equilibrium concentration of adsorbate, are usually represented by adsorption isotherms, which are essential for the practical design and critical for predicting the maximum adsorption capacity of adsorbent. Here, Langmuir, Freundlich, and Dubinin–Radushkevich (D–R) adsorption isotherm models were used to evaluate the obtained experimental data from this study.

The Langmuir adsorption isotherm assumes that adsorption takes place at specific homogeneous sites

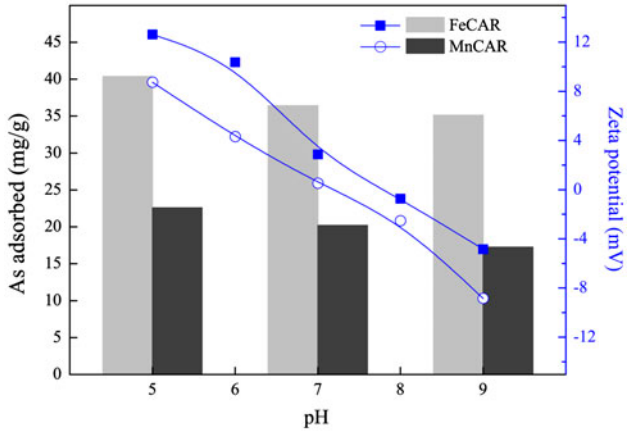

Fig. 4. Effect of pH on the adsorption of As(V) at 25˚C.

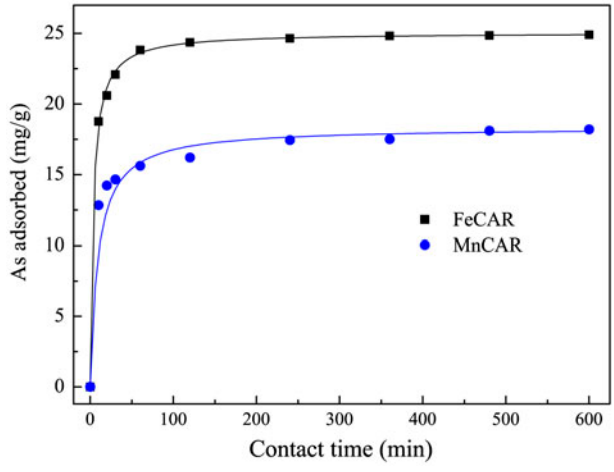

Fig. 5. Effect of contact time on the adsorption of As(V) at 25˚C.

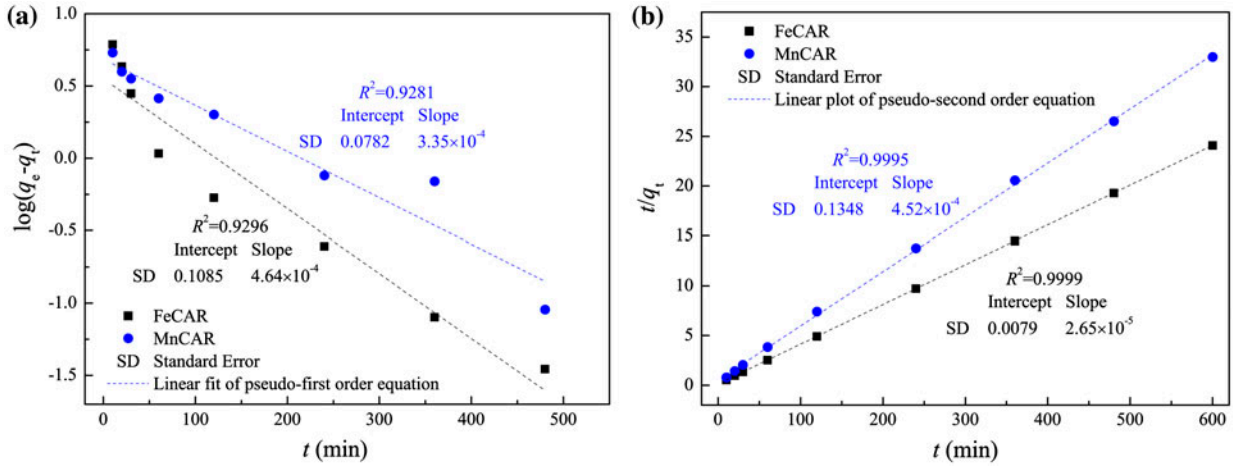

Fig. 6. Pseudo-first-order (a) and pseudo-second-order (b) kinetic plots for the adsorption of As(V) onto adsorbents at 25°C.

Table 1
Kinetic parameters for the adsorption of arsenate on FeCAR and MnCAR

		Pseudo-first-order kinetic model			Pseudo-second-order kinetic model		
Material	$q_{e,exp}$ (mg/g)	k_1 (min^{-1})	$q_{e,cal}$ (mg/g)	R^2	k_2 (g/mg min)	$q_{e,cal}$ (mg/g)	R^2
FeCAR	24.9	1.0×10^{-2}	3.54	0.9296	1.1×10^{-2}	25.1	0.9999
MnCAR	18.2	7.4×10^{-3}	4.85	0.9281	5.8×10^{-3}	18.4	0.9995

within the adsorbent and has found successful application for many adsorption processes of monolayer adsorption [20]. The linear form of this model is given by:

$$\frac{C_e}{q_e} = \frac{C_e}{q_{max}} + \frac{1}{bq_{max}} \quad (5)$$

where q_e (mg/g) is the equilibrium arsenate concentration on the adsorbent, C_e (mg/L) is the equilibrium arsenate concentration in the solution, q_{max} (mg/g) is the monolayer adsorption capacity of the adsorbent, and b (L/mg) is the Langmuir constant related to the energy of adsorption.

The type of the Langmuir isotherm can be used to predict whether the adsorption is favorable or unfavorable in terms of either the equilibrium parameter or a dimensionless constant separation factor R_L, which is represented as [21]:

$$R_L = \frac{1}{1 + bC_0} \quad (6)$$

The Freundlich adsorption isotherm assumes that the adsorption process occurs on the heterogeneous surfaces and the adsorption capacity is related to the concentration of adsorbate at equilibrium [22]. The linear form of this model is expressed as:

$$\log q_e = \log K_F + \frac{1}{n} \log C_e \quad (7)$$

where K_F (L/g) and n are Freundlich adsorption isotherm constants, being indicative of the extent of the adsorption and the degree of nonlinearity between solution concentration and adsorption, respectively.

The Dubinin–Radushkevich (D–R) adsorption isotherm [23] was employed to distinguish the adsorption of arsenate on adsorbents as physical or chemical process. The equation of this model can be written as:

$$\ln q_e = \ln q_m - \beta\varepsilon^2 \quad (8)$$

where q_m is the theoretical saturation adsorption capacity (mg/g), β is a constant correlated with the mean free energy of adsorption (mol^2/J^2), ε is the Polanyi potential, which is equal to:

$$\varepsilon = RT \ln\left(1 + \frac{1}{C_e}\right) \quad (9)$$

where R is the universal gas constant (8.3145 J/mol/K), and T is the absolute temperature in Kelvin (K). The constant β gives information about the mean free energy (E, mol^2/kJ^2) of sorption per molecule of the adsorbate when it is transferred to the surface of the solid from infinity in the solution and can be computed by:

$$E = \frac{1}{\sqrt{2\beta}} \tag{10}$$

The linear plots and isotherm constants of each model were shown in Fig. 7 and Table 2. For both FeCAR and MnCAR, the highest regression correlation coefficient was observed for Langmuir model, followed by Freundlich and D–R models, indicating that the Langmuir model was most suitable for describing the present systems. It was also proved that the formation of monolayer coverage of arsenate on the outer surface of the adsorbents. The q_{max}s calculated from Langmuir equation were 44.4 and 22.6 mg/g for FeCAR and MnCAR, respectively, which are similar to or even greater than those of other adsorbents (Table 3). Hence, the FeCAR and MnCAR could be considered as a promising alternative material to remove arsenate from real water.

The R_L value indicates the shape of the isotherm to be favorable for adsorption ($0 < R_L < 1$) or unfavorable ($R_L > 1$). The calculated R_L values in this study were estimated to 0.002–0.089 for FeCAR and 0.014–0.365 for MnCAR, which confirmed that the modified alkaline residue is favorable for arsenate adsorption. Furthermore, the n values of Freundlich equation also give an indication on the favorability of sorption. The n values were determined as 2.15 and 2.76 for FeCAR and MnCAR, respectively, indicating favorable adsorption [29].

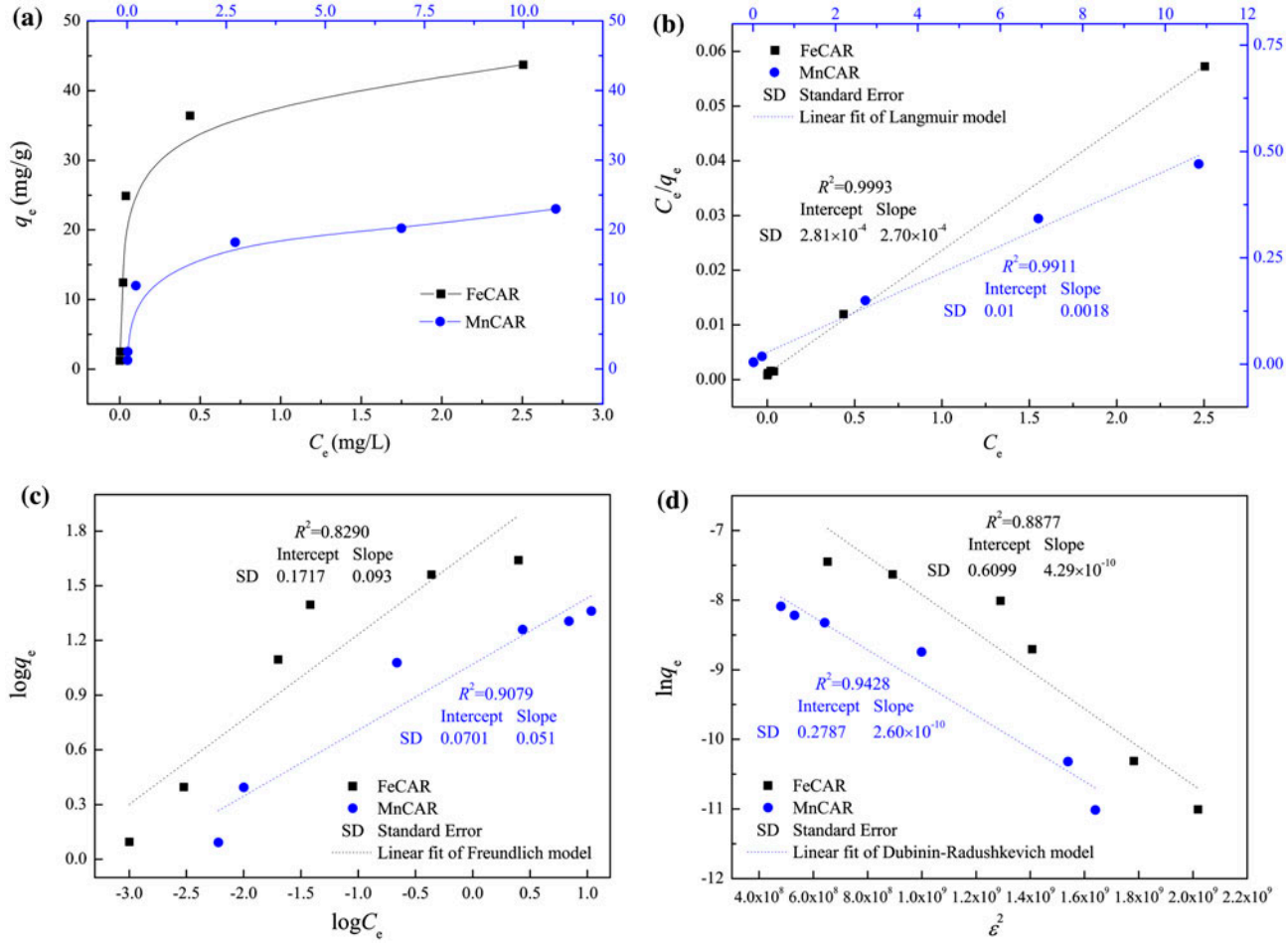

Fig. 7. (a) Adsorption isotherm of As(V) on adsorbents at 25℃, (b) Langmuir, (c) Freundlich, and (d) Dubinin–Radushkevich isotherm plots for the adsorption of As(V) on adsorbents at 25℃.

Table 2
Isotherm parameters for the adsorption of arsenate on FeCAR and MnCAR at 25℃

	Langmuir model			Freundlich model			Dubinin–Radushkevich model		
Material	q_{max} (mg/g)	b (L/mg)	R^2	K_F (mg/g (1/mg$^{1/n}$))	n	R^2	q_m (mg/g)	E (kJ/mol)	R^2
FeCAR	44.44	20.45	0.9993	50.01	2.15	0.8290	418.3	13.61	0.8877
MnCAR	22.62	3.48	0.9911	11.76	2.76	0.9079	81.47	14.43	0.9428

Table 3
Comparison of adsorption capacity (q_{max}) of various adsorbents for As(V) adsorption

Adsorbents	q_{max} (mg/g)	Refs.
FeCAR	44.44	This study
MnCAR	22.62	This study
Iron oxide amended rice husk char	1.15–1.46	[24]
Charred dolomite	2.157	[25]
Modified montmorillonite	8.85–15.15	[26]
KOH-activated carbon	26.3	[14]
Goethite-modified waste eggshell	0.919	[6]
Ferric-based layered double hydroxide	23.6	[27]
Leonardite	8.40	[28]

The magnitude of E is an important factor for estimating the main mechanism. When $E < 8$ kJ/mol, the adsorption type can be explained by physisorption, for E between 8 and 16 kJ/mol, the adsorption type can be explained by ion exchange, and if $E > 16$ kJ/mol, the adsorption type can be explained by a stronger chemisorption than ion exchange [30]. The E values obtained from Eq. (10) were 13.61 kJ/mol for FeCAR and 14.43 kJ/mol for MnCAR, which are in the sorption energy range of ion exchange reaction. This suggests that arsenate adsorption on modified alkaline residue is attributed to chemical sorption rather than physical sorption, which was in good agreement with the findings from kinetic studies.

3.5. Adsorption thermodynamics

In practical application, the thermodynamic parameters are usually used as indicators of the adsorption process. In the present system, the thermodynamic parameters of standard free energy change (ΔG°, kJ/mol), enthalpy change (ΔH°, kJ/mol), and entropy change (ΔS°, kJ/mol/K) were determined by Eqs. (11)–(13) [31] at temperatures of 25, 35, and 45℃.

$$K = \frac{C_s}{C_e} \tag{11}$$

$$\Delta G^\circ = -RT \ln K \tag{12}$$

Table 4
Thermodynamic parameters for the adsorption of arsenate on FeCAR and MnCAR (initial arsenate concentration 10 mg/L)

Material	T (℃)	ΔG° (kJ/mol)	ΔH° (kJ/mol)	ΔS° (kJ/mol/K)
FeCAR	25	−15.70		
	35	−17.49	62.38	0.26
	45	−20.96		
MnCAR	25	−4.80		
	35	−5.69	17.95	0.08
	45	−6.33		

Table 5
Effect of coexisting anions on As(V) removal (%) (initial arsenate concentration 5.0 mg/L, dosage 0.4 g/L, pH 7.2 ± 0.1)

Material	Anion concentrations (mg/L)	Anions					
		SO_4^{2-}	PO_4^{3-}	HCO_3^-	Cl^-	SiO_3^{2-}	NO_3^-
FeCAR	0	99.63	99.63	99.63	99.63	99.63	99.63
	10	99.44	64.18	99.22	99.56	76.34	99.52
	100	98.98	44.86	98.52	99.60	38.62	99.50
	500	98.28	22.52	92.37	99.42	18.78	99.38
MnCAR	0	95.60	95.60	95.60	95.60	95.60	95.60
	10	92.58	45.44	87.35	94.72	57.24	95.52
	100	89.65	19.66	79.92	92.54	16.42	92.54
	500	88.76	12.54	68.11	91.78	13.36	91.98

$$\ln K = \frac{\Delta S^\circ}{R} - \frac{\Delta H^\circ}{RT} \quad (13)$$

where K is the adsorption equilibrium constant, C_s is the equilibrium adsorption capacity (mg/g), C_e is the equilibrium concentration (mg/L), R is the ideal gas constant (8.3145 J/mol/K), and T is the temperature (K). The calculated values of thermodynamic parameters are shown in Table 4. The negative ΔG° values indicated that the adsorption of arsenate on both FeCAR and MnCAR was spontaneous. The values of ΔG° decreased with a temperature increase, suggesting that adsorption of arsenate on modified alkaline residue is an endothermic process, and the positive ΔH° could confirm this conclusion. The positive value of ΔS° revealed some structural changes might occur among arsenate and modified alkaline residue during the adsorption process, which lead to an increment in the randomness of the solid solution system.

3.6. Effect of coexisting anions

Natural inorganic anions in water could be reactive toward the surface of adsorbent, thereby influencing the removal efficiency of arsenate. The results of the competing anion studies are listed in Table 5. For FeCAR, the presence of SO_4^{2-}, Cl^-, HCO_3^-, and NO_3^- has shown negligible effect on the arsenate removal, while the PO_4^{3-} and SiO_3^{2-} caused a significant decrease in the removal efficiency of As(V). This phenomenon can be interpreted by that the phosphate, silicate, and arsenate have similar structure and chemical behavior, competing for specific adsorption sites on the surface of FeCAR. Analogous tendency could be observed for MnCAR. In addition, for MnCAR, the interference by mentioned anions was greater than FeCAR, concluding that MnCAR had a relatively lower affinity toward arsenate than FeCAR.

4. Conclusions

The experimental results showed that the modified alkaline residue could potentially be employed as an efficient adsorbent in the removal of arsenate. Modification of alkaline residue by iron could obviously enhance the arsenate adsorption ability as compared to the manganese modification. The kinetics of arsenate adsorption by FeCAR was more rapid than that of MnCAR. The pseudo-second-order kinetic model was considered as the more appropriate model to describe the whole adsorption processes for both FeCAR and MnCAR, confirming that the adsorption of arsenate was mainly controlled by chemical process. The isotherm data of the two adsorbents fitted well with the Langmuir isotherm model, and the q_{max}s calculated using the Langmuir equation were 44.4 and 22.6 mg/g for FeCAR and MnCAR, respectively, which could compete with other low-cost adsorbents. The thermodynamic study revealed that adsorption of arsenate on modified alkaline residue was a spontaneous and endothermic process. Considering the actual groundwater containing various competing ions, the common anions were selected to evaluate the performance of adsorbents, and the results showed that a relatively high concentration of phosphate and silicate causes a severely negative impact on the As(V) removal. Further investigations will focus on utilizing FeCAR and MnCAR for As-contaminated soil immobilization.

Acknowledgments

This work was financial supported by National Natural Science Foundation of China (No. 51278248) and Jiangsu Provincial education ministry of China (No. KYZZ_0129).

References

[1] A. Goswami, P.K. Raul, M.K. Purkait, Arsenic adsorption using copper(II) oxide nanoparticles, Chem. Eng. Res. Des. 90 (2012) 1387–1396.

[2] P. Chutia, S. Kato, T. Kojima, S. Satokawa, Arsenic adsorption from aqueous solution on synthetic zeolites, J. Hazard. Mater. 162 (2009) 440–447.

[3] R.Z. Chen, Z.Y. Zhang, Y.N. Yang, Z.F. Lei, N. Chen, X. Guo, C. Zhao, N. Sugiura, Use of ferric-impregnated volcanic ash for arsenate(V) adsorption from contaminated water with various mineralization degrees, J. Colloid Interface Sci. 353 (2011) 542–548.

[4] D.N. Thanh, M. Singh, P. Ulbrich, F. Štěpánek, N. Strnadová, As(V) removal from aqueous media using α-MnO_2 nanorods-impregnated laterite composite adsorbents, Mater. Res. Bull. 47 (2012) 42–50.

[5] A. Neumann, R. Kaegi, A. Voegelin, A. Hussam, A.K.M. Munir, S.J. Hug, Arsenic removal with composite iron matrix filters in Bangladesh: A field and laboratory study, Environ. Sci. Technol. 47 (2013) 4544–4554.

[6] J.S. Markovski, V. Đokić, M. Milosavljević, M. Mitrić, A.A. Perić-Grujić, A.E. Onjia, A.D. Marinković, Ultrasonic assisted arsenate adsorption on solvothermally synthesized calcite modified by goethite, α-MnO_2 and goethite/α-MnO_2, Ultrason. Sonochem. 21 (2014) 790–801.

[7] D. Mohan, C.U. Pittman, Arsenic removal from water/wastewater using adsorbents—A critical review, J. Hazard. Mater. 142 (2007) 1–53.

[8] Y.J. Tu, C.F. You, C.-K. Chang, S.L. Wang, T.S. Chan, Arsenate adsorption from water using a novel fabricated copper ferrite, Chem. Eng. J. 198/199 (2012) 440–448.

[9] Y.B. Yan, X.Y. Sun, F.B. Ma, J.S. Li, J.Y. Shen, W.Q. Han, X.D. Liu, L.J. Wang, Removal of phosphate from etching wastewater by calcined alkaline residue: Batch and column studies, J. Taiwan Inst. Chem. Eng. 45 (2014) 1709–1716.

[10] M.X. Zhu, L. Lee, H.H. Wang, Z. Wang, Removal of an anionic dye by adsorption/precipitation processes using alkaline white mud, J. Hazard. Mater. 149 (2007) 735–741.

[11] S. Şener, Use of solid wastes of the soda ash plant as an adsorbent for the removal of anionic dyes: Equilibrium and kinetic studies, Chem. Eng. J. 138 (2008) 207–214.

[12] X. Cao, L. Sun, C. Jin, Y. Gao, Y. Liu, X. You, The competitive absorption effect of heavy metals on alkaline sludge, Shandong Sci. 22 (2009) 17–20 [In Chinese].

[13] X. Cao, C. Jin, G. Peng, X. Liu, Adsorption and desorption of ammonia-nitrogen on acidified alkaline residue, Environ. Prot. Chem. Ind. 26 (2006) 259–262 [In Chinese].

[14] A.F. Hassan, A.M. Abdel-Mohsen, H. Elhadidy, Adsorption of arsenic by activated carbon, calcium alginate and their composite beads, Int. J. Biol. Macromol. 68 (2014) 125–130.

[15] X. Sun, Y. Yan, J. Li, W. Han, L. Wang, SBA-15-incorporated nanoscale zero-valent iron particles for chromium(VI) removal from groundwater: Mechanism, effect of pH, humic acid and sustained reactivity, J. Hazard. Mater. 266 (2014) 26–33.

[16] T. Kaludjerovic-Radoicic, S. Raicevic, Aqueous Pb sorption by synthetic and natural apatite: Kinetics, equilibrium and thermodynamic studies, Chem. Eng. J. 160 (2010) 503–510.

[17] Z. Ma, Q. Li, Q.Y. Yue, B.Y. Gao, W. Li, X. Xu, Q. Zhong, Adsorption removal of ammonium and phosphate from water by fertilizer controlled release agent prepared from wheat straw, Chem. Eng. J. 171 (2011) 1209–1217.

[18] Y.S. Ho, Citation review of Lagergren kinetic rate equation on adsorption reaction, Scientometrics 59 (2004) 171–177.

[19] Y.S. Ho, Review of second order models for adsorption systems, J. Hazard. Mater. 136 (2006) 681–689.

[20] M. Uğurlu, M.H. Karaoğlu, Adsorption of ammonium from an aqueous solution by fly ash and sepiolite: Isotherm, kinetic and thermodynamic analysis, Microporous Mesoporous Mater. 139 (2011) 173–178.

[21] T.W. Weber, R.K. Chakravorti, Pore and solid diffusion models for fixed-bed adsorbers, AIChE J. 20 (1974) 228–238.

[22] W. Wei, R. Sun, J. Cui, Z. Wei, Removal of nitrobenzene from aqueous solution by adsorption on nanocrystalline hydroxyapatite, Desalination 263 (2010) 89–96.

[23] M.M. Dubinin, The potential theory of adsorption of gases and vapors for adsorbents with energetically nonuniform surfaces, Chem. Rev. 60 (1960) 235–241.

[24] C.O. Cope, D.S. Webster, D.A. Sabatini, Arsenate adsorption onto iron oxide amended rice husk char, Sci. Total Environ. 488/489 (2014) 554–561.

[25] Y. Salameh, A.B. Albadarin, S. Allen, G. Walker, M.N.M. Ahmad, Chem. Eng. J. 259 (2015) 663–671.

[26] X. Ren, Z. Zhang, H. Luo, B. Hu, Z. Dang, C. Yang, L. Li, Adsorption of arsenic on modified montmorillonite, Appl. Clay Sci. 97/98 (2014) 17–23.

[27] J. Hong, Z. Zhu, H. Lu, Y. Qiu, Synthesis and arsenic adsorption performances of ferric-based layered double hydroxide with α-alanine intercalation, Chem. Eng. J. 252 (2014) 267–274.

[28] Y. Chammui, P. Sooksamiti, W. Naksata, S. Thiansem, O. Arqueropanyo, Removal of arsenic from aqueous solution by adsorption on Leonardite, Chem. Eng. J. 240 (2014) 202–210.

[29] H. Chen, J. Zhao, G.L. Dai, J.Y. Wu, H. Yan, Adsorption characteristics of Pb(II) from aqueous solution onto a natural biosorbent, fallen *Cinnamomum camphora* leaves, Desalination 262 (2010) 174–182.

[30] H. Demiral, İ. Demiral, F. Tümsek, B. Karabacakoğlu, Adsorption of chromium(VI) from aqueous solution by activated carbon derived from olive bagasse and applicability of different adsorption models, Chem. Eng. J. 144 (2008) 188–196.

[31] H. Hou, R. Zhou, P. Wu, L. Wu, Removal of Congo red dye from aqueous solution with hydroxyapatite/chitosan composite, Chem. Eng. J. 211/212 (2012) 336–342.